Coastal Engineering 186 (2023) 104404

Contents lists available at ScienceDirect

Coastal Engineering

journal homepage: www.elsevier.com/locate/coastaleng

Simple and explicit neural network-derived formula to estimate wave reflection on mound breakwaters

Pilar Díaz-Carrasco *, Jorge Molines, M. Esther Gómez-Martín, Josep R. Medina

Dept. of Transportation, Universitat Politècnica de València, Camino de Vera S/n, 46022, Valencia, Spain

ARTICLE INFO

Keywords:
Wave reflection
Mound breakwaters
Neural network
Empirical formula
Laboratory data
Modelling

ABSTRACT

The main objective of this study was to develop a new one-parameter explicit formula to estimate wave reflection on mound breakwaters under regular and irregular waves in non-overtopping and non-breaking wave conditions. The Artificial Neural Network (ANN) methodology was used to rank a list of possible explanatory variables and to identify relationships between the key explanatory variables and wave reflection. Data corresponding to 494 small-scale two-dimensional physical tests from University of Granada (UGR) and Aalborg University (AAU) were collected to apply the ANN methodology in developing the new formula. The relative water depth, h/L, being h the water depth and L the wavelength, and the seaward slope angle, $\cot\alpha$, were found to be the two main explanatory variables for the measured squared wave reflection coefficient, K_R^2. An exponential relationship between K_R^2 and $(h/L)\ /\tan\alpha$ with only one fitting identified parameter was sufficient to explain 88% of the variance for observed K_R^2 corresponding to 265 tests using regular waves from the UGR laboratory. A relationship between regular and irregular wave parameters using ANN modelling and the results of 16 tests with irregular waves from UGR was also: $H_I = 1.416\ H_{rms,I}$ and $T = 1.050\ T_{01}$; being H_I and T the incident wave height and wave period for regular waves, and $H_{rms,I}$ and T_{01} the incident root mean square wave height and spectral mean wave period for irregular waves. The new empirical formula depending only on $(h/L)\ /\tan\alpha$ explained 91% of the variance for measured K_R^2 of 213 additional tests with irregular waves from the AAU laboratory. The new formula was calibrated and validated using physical models with rock and concrete armor units, several seaward slope angles, water depths, and core permeability. The new one-parameter empirical formula showed a better agreement than other simple empirical formulas given in the literature and explained more than 65% of the variance for K_R^2 observations from a general database used for comparison.

1. Introduction

The main functions of any breakwater are to protect harbors, coastal regions or navigation channels from wave action. The mound breakwater is the most frequently used breakwater typology in the world due to its ability to dissipate the wave energy, its relatively simple design and the possibility of being constructed using different rock and large concrete armor units. Breakwaters must be designed to provide safety and service in coastal areas and harbors during a given lifetime. The hydraulic performance of these maritime structures is calculated considering the dissipated, transmitted and reflected wave energy which may significantly affect the waves in the vicinity of the structure. Wave reflection from breakwaters may influence beaches and ship navigation in harbors due to dangerous and extreme wave conditions, and may compromise the structure stability due to the induced scour at the structure toe. These problems will become more frequent and will have a greater impact in the future given climate change, sea level rise and potentially stronger wave storms (Camus et al., 2019). The challenges to protect coasts and harbors from the effects of climate change as well as the need for a correct estimation of reflected energy from coastal structures, means more accurate and easy-to-apply design formulas for mound breakwaters are required.

Several empirical formulas found in the literature to predict wave reflection characterized by the reflection coefficient, K_R (ratio between the reflected and incident wave height), are based on the seminal work of Battjes (1974), who proposed using the Iribarren number (Iribarren and Nogales, 1949), $\xi_0 = \tan\alpha/\sqrt{2\pi H_{m0,I}/gT_p^2}$ (being $H_{m0,I}$ the significant spectral incident wave height and T_p the peak wave period) as the

* Corresponding author.
E-mail address: pdiacar@upv.es (P. Díaz-Carrasco).

https://doi.org/10.1016/j.coastaleng.2023.104404
Received 1 June 2023; Received in revised form 22 September 2023; Accepted 1 October 2023
Available online 8 October 2023

dynamic similarity parameter to analyze wave energy transformation on breakwaters and to identify wave breaker types on the slope. Since then, most explicit wave reflection formulas are combinations of the Iribarren number with calibrated coefficients and dimensionless variables selected on empirical grounds (Zanuttigh and Van der Meer, 2008). These studies considered an extensive experimental database tested with a variety of wave conditions, types of structures, measurement devices and techniques which are specific for each laboratory. In some cases, K_R was measured in research studies focusing on hydraulic stability, wave overtopping or wave transmission (Van der Meer, 1988; Lykke Andersen and Burcharth, 2004; Pearson et al., 2004). The consequence of this variety of methods is a high uncertainty in the results and thus inaccurate wave reflection estimations and explicit empirical formulas valid only for very limited ranges.

Over the last two decades, new empirical formulas, complex estimators and numerical models have been used to achieve more accurate predictions for wave reflection. Besides reflection formulas based on the Iribarren number, Benedicto (2004), Clavero et al. (2018) and others analyzed the influence of other variables, such as the relative water depth, h/L or h/L_0, in which h is the water depth, L is the wavelength at the toe of the structure calculated with the mean wave period and L_0 is the deep water wavelength calculated with the peak period. Authors such as Vílchez et al. (2016) and Díaz-Carrasco et al. (2021) developed more complex explicit empirical formulas with better agreement using several fitting parameters. In the numerical field, several studies analyzed wave energy transformation on coastal structures by depth-integrated models based on Non-Linear Shallow Water Equations and Boussinesq equations (Wurjanto and Kobayashi, 1993) or Reynolds Averaged Navier Stoke equations (Lara et al., 2006); however, these numerical models are computationally time-consuming and may overestimate the wave reflection results on coastal structures (Zanuttigh et al., 2009). Wave reflection is also estimated using Artificial Neural Network (ANN) models, which are complex multi-parametric formulas that offer greater accuracy and low computational cost. The use of ANN makes possible to include many input variables and to establish relationships between them and between the output variable from complex fitting formulas with weight-weighted of the input variables. The correlations made by ANN between the main input and output variables are not intuitive, have many fitting parameters and are difficult to obtain and represent without using the ANN model as a toolbox itself. These alternatives models, such as ANN models, significantly improve the predictions for reflected wave energy on breakwaters, but they provide formulas which are extremely complex and require many fitting parameters.

In order to find an easy-to-apply method to estimate wave reflection on conventional mound breakwaters, this study develops a new simple explicit formula with only one fitting parameter and one explanatory variable valid for non-overtopping and non-breaking wave conditions. For that, the ANN benefits of weighting and correlation between input and output variables are used as a method to (1) select the main explanatory variables influencing wave reflection and (2) to obtain a simple and explicit relationship between these variables and reflected wave energy by ANN estimations. The new formula is proposed for regular and irregular waves as relationships of the wave height and wave period between regular and irregular waves were obtained. Results from 265 regular and 16 irregular tests conducted at the University of Granada (UGR), detailed by Díaz-Carrasco (2019), and Díaz-Carrasco et al. (2020), were used to calibrate the new formula. The results from 213 irregular tests carried out at Aalborg University (AAU), detailed by Eldrup et al. (2019), Eldrup and Lykke Andersen (2019a), and Díaz-Carrasco et al. (2021), were used to validate the new formula. Using the database of Zanuttigh et al. (2013), the new empirical formula was compared to other explicit simple formulas given in the literature.

This paper is structured as follows. Section 2 includes a review of the literature on wave reflection and empirical formulas used to estimate the wave reflection coefficient on mound breakwaters. Section 3 describes a list of possible explanatory variables for reflected wave energy on mound breakwaters based on variables found in the literature and the dimensional analysis detailed in Díaz-Carrasco et al. (2020). Section 4 describes the experimental data collected at UGR and AAU used to calibrate and to validate the new formula. In Section 5, an Artificial Neural Network (ANN) technique is used to select the key explanatory variables and to develop explicit estimators for wave reflection. The new wave reflection formula for mound breakwaters is described in Section 6, and it is compared with other simple empirical formulas given in the literature. Finally, Section 7 presents the conclusions derived from this study.

2. Literature review on wave reflection on mound breakwaters

Several prediction formulas can be found in the literature to estimate wave reflection on mound breakwaters, from simple explicit formulas to complex multi-parametric formulas based on ANN models. This section describes a selection of the formulas to predict wave reflection on mound breakwaters, with special attention being given to the application range of such formulas and their complexity (number of explanatory variables and fitting parameters). Fig. 1 provides a scheme of the cross-section of a mound breakwater with the main structural and wave parameters involved in wave reflection formulas used throughout this study. Table 1 offers a brief description of these formulas including the main explanatory variables, the number of fitting parameters, the armor type and core, the seaward slope angle and the tested wave conditions.

For rubble mound breakwaters, Numata (1976) first developed a 3-parameter empirical formula to estimate wave reflection for permeable breakwaters that depends on the relative breakwater width, B_s/h, B_s being the breakwater width at still water level, and the relative water depth, h/L_{01} (Eq. 1). Losada and Giménez-Curto (1981) proposed an exponential model for K_R from tests with regular waves based on the Iribarren number, defined here as, $\xi = \tan\alpha/\sqrt{2\pi H_I/gT^2}$, in which H_I and T represent the incident wave height and wave period for regular waves, respectively; this formula has 2 parameters that depend on the armor unit type (Eq. 2). Seelig and Ahrens (1981) calibrated their formula based on the Iribarren number, $K_R = \mathrm{f}\,(\xi_0 = \tan\alpha/\sqrt{2\pi H_{m0,I}/gT_p^2})$, being $H_{m0,I}$ the significant spectral incident wave height and T_p the peak wave period, from smooth slopes to rough slopes and re-fitted the 2 parameters as a function of the armor layer composition (Eq. 3). Postma (1989) developed a formula to consider the effect of the core permeability in the estimation of $K_R = \mathrm{f}\,(\xi_0)$ with 2 parameters (Eq. 4). In this line, Van der Meer (1992) improved the formula given by Postma (1989) with more accurate calculations and introduced the notational permeability factor, P, to consider the armor/core composition and number of layers; this is a 4-parameter formula (Eq. 5). Davidson et al. (1996) collected full-scale measurements from rock island breakwaters and developed a prediction scheme to estimate wave reflected energy. This estimation weighs the contributions of deep water wavelength, L_0, significant spectral incident wave height, $H_{m0,I}$, water depth, h, seaward slope angle, α, and the nominal diameter of the main armor layer, $D_{n50,a}$ (Eq. 6). Finally, to improve the wave reflection predictions based on the Iribarren number, Zanuttigh and Van der Meer (2008) noted that the spectral energy wave period, $T_{-1,0}$, is useful to represent bi-modal spectra or flat spectra for shallow water. These authors refitted the 2-parameter formula given by Seelig and Ahrens (1981), as a function of the slope type and the armor units, using $T_{-1,0}$ in the expression of the Iribarren number as $\xi_{-1,0} = \tan\alpha/\sqrt{2\pi H_{m0,I}/gT_{-1,0}^2}$. They also developed a new improved formula for K_R based on the spectral Iribarren number, $\xi_{-1,0}$, with 2 parameters that depend on the slope composition of the breakwater (Eq. 7) and can be extended to structures with berms or subjected to oblique waves (Zanuttigh and Lykke Andersen, 2010).

Over the last two decades, several studies have questioned the relevance of the Iribarren number to explain K_R and focused on developing

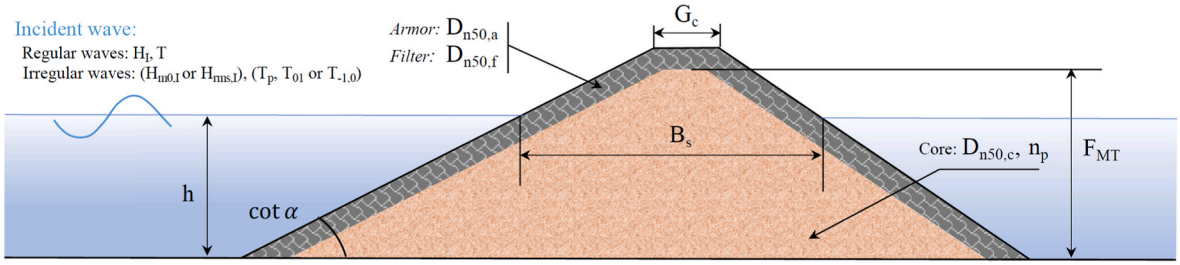

Fig. 1. Cross-section of a mound breakwater with the main structural and wave parameters used in this study.

Table 1
Prediction formulas found in the literature to estimate wave reflection on mound breakwaters.

Reference	*Eq.*	*Explanatory variables*	*# Param.*	*Armor + core permeability*	*Slope angle (cot α)*	*Wave conditions*
$K_R^2 = a(B_s/h)^{b(h/L_{01})+c}$ Numata (1976)	(1)	$B_s/h/L_{01}$	3	Rock + permeable	[1, 1.3]	Irregular
Losada and Giménez-Curto (1981) $K_R = a(1 - e^{b\xi})$	(2)	$\xi = \tan\alpha/\sqrt{2\pi H_I/gT^2}$	2	Dolos + permeable Rock + permeabl	[1.5, 3]	Regular
Seelig and Ahrens (1981) $K_R = \frac{a\xi_0^2}{b+\xi_0^2}$	(3)	$\xi_0 = \tan\alpha/\sqrt{2\pi H_{m0,I}/gT_p^2}$	2	Rock + impermeable Rock + permeable Concrete + permeable	[1.5, 4]	Regular and irregular
Postma (1989) $K_R = 0.14\cdot\xi_{50}^{0.73}$	(4)	$\xi_0 = \tan\alpha/\sqrt{2\pi H_{m0,I}/gT_p^2}$	2	Rock + impermeable Rock + permeable	[1.5, 6]	Irregular
Van der Meer (1992) $K_R = 0.071P^{-0.082}\tan\alpha^{0.62}\left(\frac{H_{m0,I}}{L_0}\right)^{-0.46}$	(5)	$\tan\alpha$ P $H_{m0,I}/L_0$	4	Rock + permeable	[1.5, 3]	Irregular
Davidson et al. (1996) $K_R = \frac{0.10h^{0.06}L_0^{0.36}}{H_{m0,I}^{0.12}\cot\alpha^{0.15}}$	(6)	- h - L_0 - $H_{m0,I}$ - cot α	5	Rock + permeable	[0.82, 1.55]	Irregular
Zanuttigh and Van der Meer (2008) $K_R = \tanh(a\xi_{-1,0}^b)$	(7)	$\xi_{-1,0} = \tan\alpha/\sqrt{2\pi H_{m0,I}/gT_{-1,0}^2}$	2	Concrete + permeable Rock + permeable Rock + impermeable	[1.5, 4]	Regular and irregular
Muttray et al. (2006) $K_R = \frac{1}{1.3+3\cdot(2\pi h/L_0)}$	(8)	h/L_0	2	Accropode™ + permeable	1.5	Regular and irregular
Calabrese et al. (2010) $K_R = f(\tan\alpha, h/L_0, H_{m0,I}/L_0, P)$	(9)	$\tan\alpha$ h/L_0 P: permeability factor $H_{m0,I}/L_0$	8	Ecopode™+permeable	[1.33, 1.5]	Irregular
Medina and Gómez-Martín (2016) $K_R = \frac{1}{\sqrt{20\cdot(2\pi h/L_0 - 0.5)}}$	(10)	h/L_0	2	Cubipod® + permeable	1.5	Irregular
Zanuttigh et al. (2013) ANN multi-parametric formula		13 variables (inputs)	601	Rock + permeable Rock + impermeable Concrete + permeable	[0–7]	Irregular
Vílchez et al. (2016) $K_R = (K_{R1} - K_{R0})\left[1+\left(\frac{A_{eq}/L^2}{a}\right)^{\gamma}\right]^{-1} + K_{R0}$; K_{R1} and K_{R0} the upper and lower asymptotes, respectively	(11)	$A_{eq}/L_{01}{}^2$	4	Rock + permeable Cube + permeable	1.5	Irregular
Díaz-Carrasco et al. (2021) $K_R = (K_{R1} - K_{R0})\left[1+\left(\frac{h/L_{-1,0}}{a}\right)^{\gamma}\right]^{-1} + K_{R0}$; K_{R1} and K_{R0} the upper and lower asymptotes, respectively	(12)	$h/L_{-1,0}$	4	Rock + permeable Cube + permeable	[1.5, 3]	Irregular
This study $K_R^2 = \exp\left[-8\left(\frac{h/L_{01}}{\tan\alpha}\right)\right]$	(19)	$\frac{h/L_{01}}{\tan\alpha}$	1	Rock + permeable Cube + permeable	[1.5, 3]	Regular and irregular

new explicit formulas based on parameters other than the Iribarren number. First, Muttray et al. (2006) proposed an empirical formula with 2 parameters that relates the wave reflection coefficient for concrete unit armored mound breakwaters ($\cot\alpha = 1.5$) with only one explanatory variable, h/L_0, the relative water depth (Eq. 8). Later, Calabrese et al. (2010) developed a more complex formula with 8 parameters for wave reflection on a breakwater with concrete armor units. The main variables for their formula are the relative water depth, h/L_0, the

seaward slope angle, α, the incident wave steepness, $H_{m0,I}/L_0$, and the notional permeability factor, P (Eq. 9). Lastly, Medina and Gómez-Martín (2016) proposed a wave reflection formula for single- and double-layer Cubipods® armors on a slope $\cot\alpha = 1.5$ with one explanatory variable, h/L_0, and 2 parameters (Eq. 10).

The multiparametric Artificial Neural Network (ANN) model developed by Zanuttigh et al. (2013) provides estimations for wave reflection coefficients from a wide range of coastal and harbor structures, from rock permeable straight slopes to seawalls and including oblique wave attack conditions. This ANN model is usually more accurate than simple explicit empirical formulas, but it calculates complex multi-parametric formulas with a large number of explanatory variables, parameters and complex functional relationships. Vílchez et al. (2016) defined the scattering parameter, $A_{eq}/\ L_{01}^2$, being $A_{eq} \approx B_s \bullet h$, the core area under the still water level, and fitted a sigmoidal function with $A_{eq}/\ L_{01}^2$ to the laboratory data of wave energy transformation on various breakwater typologies (Eq. 11). Díaz-Carrasco et al. (2020) analyzed the wave energy transformation processes in the laboratory by applying a dimensional analysis, and they defined a new similarity parameter $\chi = (h/L_{01})(H_{m0,I}/L_{01})$, which identifies the regions of wave energy transformation (reflected, dissipated and transition). Díaz-Carrasco et al. (2021) proposed an explicit formula with sigmoidal functions and only one explanatory variable, $h/L_{-1,0}$, being $L_{-1,0}$ the wavelength calculated with the spectral energy period, $T_{-1,0}$, but the sigmoidal functions require 4 parameters for each tested slope angle to achieve satisfactory results (Eq. 12).

Table 1 provides a list of selected formulas found in the literature to estimate the wave reflection on mound breakwaters. The structural and wave parameters included in Table 1 were defined throughout this Section 2. For regular waves, the wave parameters in Table 1 refer to H_I incident wave height, T wave period, L and L_0 wavelength at the toe of the structure and deep water wavelength, respectively, both calculated with T. For irregular waves, the wave parameters refer to $H_{m0,I}$ significant spectral incident wave height; T_p, T_{01}, $T_{-1,0}$ peak, spectral mean and spectral energy wave period; L_{01} wavelength at the toe of the structure calculated with the spectral mean wave period, T_{01}, and L_0 deep wavelength calculated with the peak wave period, T_p.

Existing formulas predict wave reflection on mound breakwaters, but many of them have been designed based on laboratory tests with specific conditions, instruments and techniques of analysis (e.g., the method to separate incident and reflected waves) and have significant experimental scatter in their results. Some formulas fit most observations very well, but these use complex functions and many fitting parameters that depend on the composition and the slope angle of the structure. In this study, the 2-parameter formulas found in the literature were selected to compare with the simpler 1-parameter empirical formula developed in this study.

3. Explanatory variables affecting wave reflection on mound breakwaters

This study considered eleven dimensionless variables as candidate explanatory variables that may influence wave reflection on mound breakwaters with straight slopes under non-overtopping and non-breaking wave conditions (see Fig. 1). In the eleven explanatory variables and hereafter, the wave parameters for incident wave height, wave period and wavelength indicated here as H, T and L, respectively, refer in this study to H_I, T and L at the toe of the structure (calculated with T) for regular waves, and $H_{rms,I}$ root mean square incident wave height, T_{01} spectral mean wave period, and L_{01} wavelength at the toe of the structure (calculated with T_{01}) for irregular waves. The $H_{rms,I}$ is the wave height for irregular waves as it is related with the same energy to the wave height of regular waves.

The explanatory variables are grouped in the following five sets.

3.1. Wave variables

- $X_1 = h/L$: relative water depth at the toe of the structure,
- $X_2 = H/L$: incident wave steepness at the toe of the structure, and
- $X_3 = H/h$: relative wave height.

3.2. Core variables

- $X_4 = B^*/L$: relative characteristic width of the core, in which $B^* = G_C + 0.5F_{MT}\cot\alpha$, where G_c is the crest width and F_{MT} is the breakwater height (Kortenhaus and Oumeraci, 1998),
- $X_5 = D_{n50,c}/L$: relative core diameter, and
- $X_6 = R_{e,c} = D_{n50,c}U/\nu$: grain Reynolds number, being $U \approx n_p H/T$ the characteristic seepage velocity in the core with n_p porosity.

3.3. Armor layer variables

- $X_7 = D_{n50,a}/L$: relative armor diameter, and
- $X_8 = R_{e,Da} \approx \sqrt{gH_I}D_{n50,a}/\nu$: armor Reynolds number.

3.4. .Slope angle

- $X_9 = \cot\alpha$: seaward slope angle.

3.5. Other explanatory variables

- $X_{10} = \xi = \tan\alpha/\sqrt{H/L}$: the Iribarren number, which is selected for its use in wave reflection formulas,
- $X_{11} = \chi = (h/L)(H/L)$: the similarity parameter defined by Díaz-Carrasco et al. (2020), which identifies the regions of wave energy transformation.

X_1 and X_2 gather the wave conditions that impact the breakwater. X_3 represents the incident wave train with the same wave breaking conditions at the toe of the structure (Losada and Giménez-Curto, 1981). Under non-breaking wave conditions, $X_3 < 0.55$ (Riedel and Byrne, 1986; CIRIA/CUR/CETMEF, 2007). X_4 indicates the saturation regime of the structure (Requejo et al., 2002). X_5 governs the flow dissipation inside the core (Pérez-Romero et al., 2009), and $X_6 = R_{e,c}$ characterizes the hydrodynamic regime inside the core (Gu and Wang, 1991; Van Gent, 1995; Burcharth and Andersen, 1995). X_7 and X_8 govern the turbulence regime on the slope due to breaking and dissipation of the wave train with the armor layer (Clavero et al., 2018, 2020). When a mound breakwater is composed completely of homogeneous and permeable material, $D_{n50,a} = D_{n50,c}$, then $X_7 = X_5$. For impermeable core $D_{n50,c} = 0$. Variables X_1 to X_9 were selected following the dimensional analysis described in detail by Díaz-Carrasco et al. (2020), which includes variables of the wave train, core and armor layer that influence wave energy transformation on mound breakwaters. X_{10} and X_{11} were considered as explanatory variables for their inclusion in existing formulas to estimate wave reflection (see Section 2). The eleven explanatory variables are the input variables of the ANN models developed as simulators to ranking the candidate explanatory variables influencing wave reflection (see Section 5). The ANN method allows not only to obtain a ranking of the explanatory variables but also to obtain correlations between them. Even if the list of variables in as input variables have correlations between them, for example X_{10} and X_{11}, the ANN will choose those that best fit the output variable, whether they are independent or not.

In this study, the wave reflection on coastal structures is calculated by the squared reflection coefficient, K_R^2, which is a ratio between the total reflected (E_R) and incident (E_I) energy,

$$K_R^2 = \frac{E_R}{E_I} = \frac{\frac{1}{8}\rho g L H_R^2}{\frac{1}{8}\rho g L H^2} = \frac{H_R^2}{H^2} \tag{13}$$

where H and H_R represent the incident ($H = H_I$ for regular waves and $H = H_{rms,I}$ for irregular waves) and reflected ($H_R = H_R$ for regular waves and $H_R = H_{rms,R}$ for irregular waves) wave height, respectively; L is the local wavelength equal for both reflected and incident wave trains assuming Linear Theory, ρ is the water density, and g is the gravity acceleration.

4. Database of wave reflection on mound breakwaters

Two-dimensional (2D) physical tests from the University of Granada (UGR) and Aalborg University (AAU) were considered to develop and validate, through blind testing, the new formula proposed in this study. The results were collected from mound breakwater models with straight slopes under non-overtopping and non-breaking wave conditions. Table 2 provides the ranges of the candidate explanatory variables and wave conditions tested at the two laboratories. In Table 2, for regular waves, the wave parameters refer to $H = H_I$ incident wave height, $T = T$ wave period, and $L = L$ wavelength at the toe of the structure calculated with T. For irregular waves, the wave parameters refer to $H = H_{rms,I}$ root mean square incident wave height, $T = T_{01}$ spectral mean wave period, and $L = L_{01}$ wavelength at the toe of the structure calculated with T_{01}.

4.1. Database to develop the new formula

Experimental test results from the UGR related to wave energy transformation on mound breakwaters were considered in this study to analyze the relationship between the explanatory variables and the reflection coefficient. The UGR dataset included 281 experimental tests with three types of mound breakwaters (see Table 2): (A) 106 tests with rock homogenous mound breakwaters, $D_{n50,a} = D_{n50,c} = 30$ mm, with two seaward slope angles and two crest widths, described in Díaz-Carrasco (2019); (B) 159 tests with conventional mound breakwaters with a double-layer cube armor, $D_{n50,a} = 40.9$ mm, and a permeable core, $D_{n50,c} = 12$ mm, without filter layer, described in Díaz-Carrasco et al. (2020); and (C) 16 tests with a rock homogenous mound breakwater, $D_{n50,a} = D_{n50,c} = 30$ mm, described in Díaz-Carrasco (2019). The reference scales for cube armored models and rock armored models are 1:50 and 1:25, respectively.

From the 281 UGR tests, 265 were conducted with regular waves (H_I, T, L), and these were used to calibrate the new formula. The remaining 16 tests were conducted with irregular waves ($H_{rms,I}$, T_{01}, L_{01}), and these were used to estimate the appropriate statistical relationship of wave height and wave period to apply the new formula to irregular waves. Incident and reflected wave trains were separated by applying the method of Baquerizo (1995) based on Mansard and Funke (1987).

4.2. Database to validate the new formula

A total of 257 experimental tests from the AAU was used to validate the new wave reflection formula in a blind test: (D) 78 tests with rubble mound breakwaters with two armor unit types (double-layer rock, $D_{n50,a} = 43.9$ mm, and cube armors, $D_{n50,a} = 40.0$ mm), a filter layer, $D_{n50,f} = 15$ mm, and a permeable core, $D_{n50,c} = 5.8$ mm, described in Díaz-Carrasco et al. (2021); (E) 95 tests with mound breakwaters with a double-layer rock armor, $D_{n50,a} = 43.9$ mm, and different compositions of the core (permeable $D_{n50,c} = 5.8$ mm and 15 mm, or impermeable, $D_{n50,c} = 0$ mm) and filter layers, $D_{n50,f} = 15$ mm, described in Eldrup et al. (2019b); and (F) 40 tests of mound breakwaters with a double-layer rock armor, $D_{n50,a} = 43.9$ mm, and a permeable core, $D_{n50,c} = 15$ mm, without a filter layer, described in Eldrup and Lykke Andersen (2019a). The reference scales for cube armored models and rock armored models are also 1:50 and 1:25, respectively.

Only irregular waves were tested at AAU. The method described by Eldrup and Lykke Andersen (2019b) was applied to calculate the incident and reflected wave spectra and the time domain of incident and reflected wave trains using WaveLab3 software package (Aalborg University, 2015).

4.3. Estimation of wave reflection with formulas given in the literature

Fig. 2 illustrates the performance of the 2-parameter reflection formulas given in Table 1 (Eqs. 2, 3, 4, 7, 8 and 10). No existing formulas completely fulfill the range of the UGR and AAU tests; however, they were applied to evaluate the performance of the simplest existing $\boldsymbol{K_R^2}$ estimators. The coefficient of determination, R^2, was used in this study to measure the goodness of fit of each formula. The higher R^2, the better the estimation of $\boldsymbol{K_R^2}$.

$$R^2 = 1 - \frac{\sum_{i=1}^{N} (Y_{Mi} - Y_{Ei})^2}{\sum_{i=1}^{N} (Y_{Mi} - \overline{Y_M})^2} = 1 - \frac{MSE(Y_M)}{Var(Y_M)} \tag{14}$$

where sub-indexes E and M refer to estimated and measured data, respectively; $Y = K_R^2$ is the analyzed variable (squared reflection coefficient), $\overline{Y_M}$ is the mean value of the measured K_R^2, N is the total number of data, i is the data index (i = 1, 2, …N), MSE is the mean-squared error, and Var(Y_M) is the variance of the measure data.

Table 2
Range of variables in datasets corresponding to University of Granada (UGR) and Aalborg University (AAU).

Variable	A-UGR Díaz-Carrasco (2019)	B-UGR Díaz-Carrasco et al. (2020)	C-UGR Díaz-Carrasco (2019)	D-AAU Díaz-Carrasco et al. (2021)	E-AAU Eldrup et al. (2019b)	F-AAU Eldrup and Lykke Andersen (2019a)
	calibration	calibration	calibration	validation	validation	validation
h/L	[0.068, 0.272]	[0.05, 0.272]	[0.078, 0.313]	[0.074, 0.262]	[0.055, 0.197]	[0.053, 0.292]
H/L	[0.01, 0.044]	[0.008, 0.044]	[0.017, 0.094]	[0.014, 0.052]	[0.014, 0.056]	[0.012, 0.045]
H/h	[0.063, 0.261]	[0.044, 0.289]	[0.042, 0.241]	[0.086, 0.319]	[0.211, 0.415]	[0.129, 0.437]
B^*/L	[0.111, 0.536]	[0.085, 0.536]	[0.153, 0.618]	[0.128, 0.723]	[0.0560, 0.313]	[0.074, 0.305]
Core permeability $D_{n50,c}/L$	Permeable [0.005, 0.02]	Permeable [0.001, 0.02]	Permeable [0.006, 0.024]	Permeable [0.001, 0.01]	Permeable Impermeable [0, 0.006]	Permeable [0.002, 0.008]
$R_{e,c}$	[366.7, 938.7]	[49.77, 938.7]	[402.7, 956.5]	[57.10, 560.13]	[0, 610.67]	[152.83, 470.7]
Armor unit type $D_{n50,a}/L$	Rock [0.005, 0.02]	Cube [0.005, 0.028]	Rock [0.006, 0.024]	Rock/Cube [0.008, 0.029]	Rock [0.005, 0.017]	Rock [0.006, 0.025]
$R_{e,Da}$	[14, 875, 30, 385]	[14, 875, 43, 596]	[14, 925, 30, 575]	[24, 530, 43, 596]	[44, 682, 62, 619]	[33, 926, 49, 480]
$cot\ \alpha$	[1.5, 2]	2	2	[1.5, 3]	[1.5, 3]	[1.5, 2]
ξ	[2.388, 6.405]	[2.392, 6.405]	[3.848, 6.285]	[1.475, 5.624]	[1.437, 5.485]	[2.438, 5.952]
χ	[0.0008, 0.012]	[0.0004, 0.012]	[0.001, 0.029]	[0.001, 0.012]	[0.0008, 0.01]	[0.001, 0.011]
h (m)	0.4	0.4	0.4	0.4	0.5	0.4, 0.55, 0.6, 0.64, 0.7
Number of tests - wave conditions	106 - Regular	159 - Regular	16 - Irregular	78 - Irregular	95 - Irregular	40 - Irregular

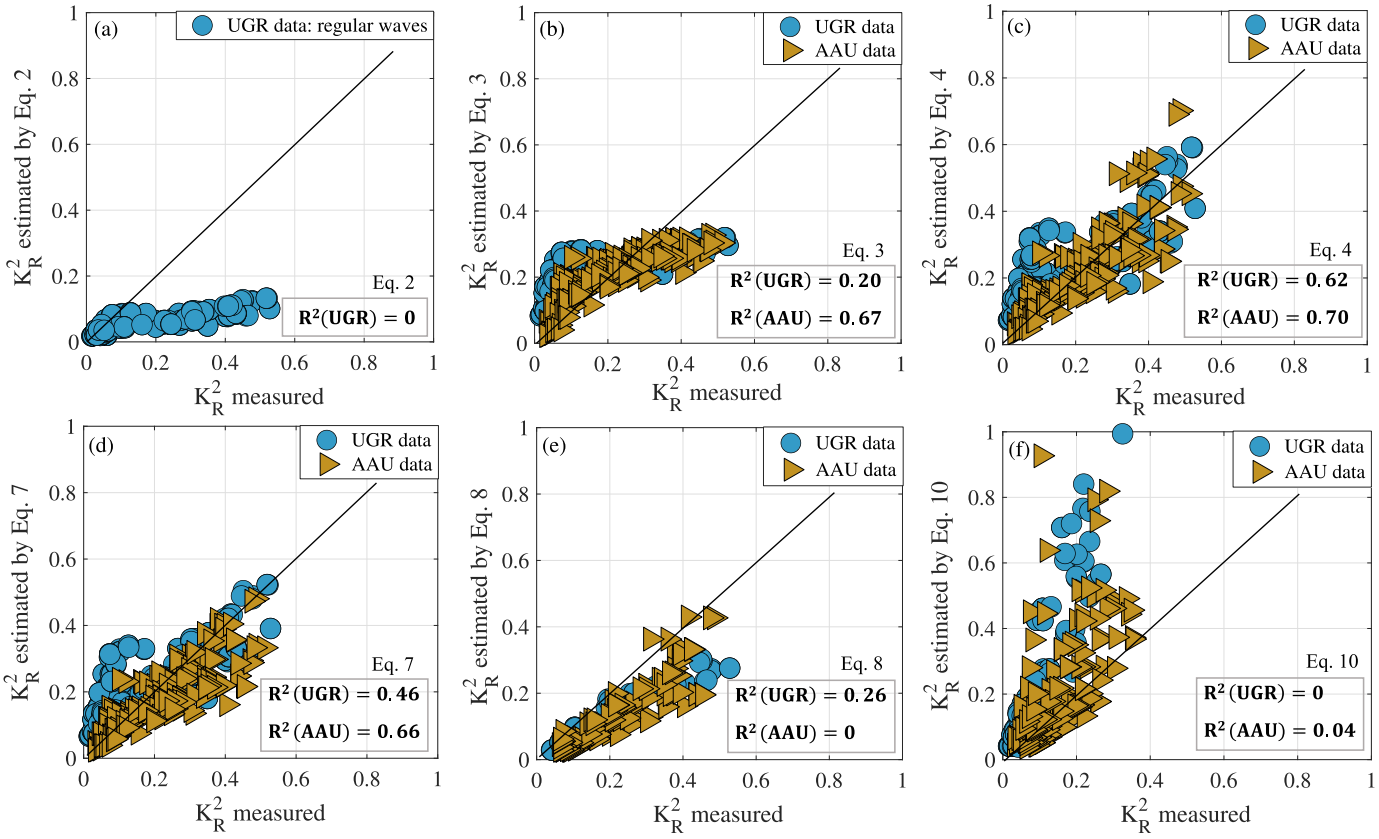

Fig. 2. Comparison between measured and estimated K_R^2 by 2-parameter reflection formulas (Eqs. 2, 3, 4, 7, 8 and 10 in Table 1).

For the UGR dataset, Eqs. 2, 3, 4, 7, 8 and 10 (Table 1) give poor estimations of K_R^2 (see Fig. 2); the best agreement is given by Eq. 4 (Postma, 1989) for double-layer rock and cube armors. For the AAU dataset, the agreements to the formulas are significantly improved and the best agreement is also given by Eq. 4 (Postma, 1989). The poor estimations of K_R^2 for some of these formulas considering the UGR and AAU datasets may be partly due to the application of such formulas outside their calibration range. For example, Eq. 2 b y Losada and Giménez-Curto (1981) was applied to cube armor (regular waves of UGR dataset), which were not tested in their study; Eq. 3 b y Seelig and Ahrens (1981) and Eq. 7 b y Zanuttigh and Van der Meer (2008) have a low R^2 value for the regular waves of UGR dataset because the fitting parameters used in their studies were calibrated mainly for irregular waves; Eq. 8 b y Muttray et al. (2006) underestimates K_R^2 values for both UGR and AAU datasets as their wave reflection formula was tested only for Accropode™ armor; and Eq. 10 b y Medina and Gómez-Martín (2016) overestimates K_R^2 values as their wave reflection formula was tested only for Cubipod® armor.

5. Methodology to develop the new empirical formula using Artificial Neural Network models

Artificial Neural Network (ANN) models are frequently used to model complex nonlinear relationships between explanatory variables (input) and response variables (output), such as wave overtopping Van Gent et al. (2007) within the CLASH European project (De Rouck and Geeraerts, 2005; EurOtop et al., 2016; Formentin et al., 2017) or wave reflection (Zanuttigh et al., 2013). As the relationships between input and output variables are not intuitive and easy to see with ANN models, they can be used as simulators to estimate explicit relationships between input and output variables and thereby to develop empirical formulas for wave reflection (Garrido and Medina, 2012), wave overtopping (Molines and Medina, 2016; Mares-Nasarre et al., 2021) or wave forces on crown walls (Molines et al., 2018). Thus, the methodology for this study is based on using ANN models as simulators to (1) identify the relevant explanatory variables within the input variables that influence the output variable, and (2) to obtain explicit relationships between the explanatory and output variables to develop a new simple empirical formula.

5.1. *Methodology to obtain the relevant explanatory variables influencing wave reflection*

In this study, a methodology similar to that developed by Molines et al. (2018) to select the relevant explanatory variables is used. An ANN model was structured with one input layer up to eleven neurons ($N_I = 1$ to 11), referring to each of the eleven candidate explanatory variables in Section 3 (X_1 to X_{11}), one hidden layer with fifteen neurons ($N_H = 15$) and one output neuron ($N_O = 1$), which is the squared reflection coefficient (K_R^2). Fig. 3 shows the scheme of the ANN structure named $I_{N_I}H_{N_H}O_{N_O}$. ANN structures were built in the MATLAB environment (see MATLAB, 2022) with the following characteristics:

(1) Early stopping criterion to lead rapid interruption of the training process (to prevent overlearning),
(2) Random selection of data division in 70% training (T_r), 15% validation (V) and 15% test (T_s),
(3) Levenberg-Marquardt training algorithm and,
(4) Hyperbolic tangent sigmoid transfer function for hidden neurons.

As indicated above, the data used in the ANN model to identify relationships between the explanatory variables and the squared wave reflection coefficient were the 265 regular tests conducted in the UGR (see Table 2). The number of free parameters in each ANN model is given

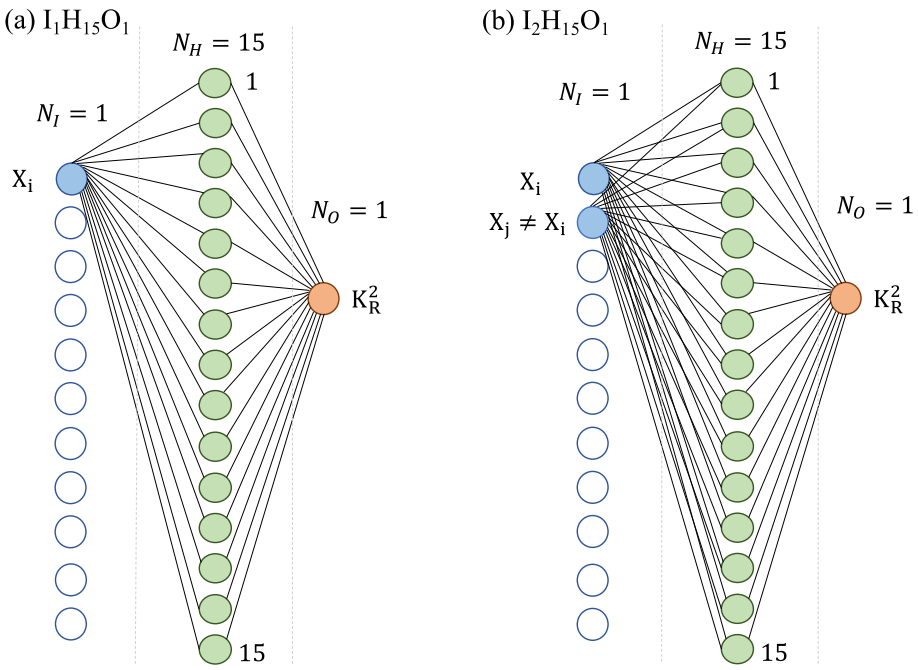

Fig. 3. Structure of the two ANN models used as simulators: (a) $I_1H_{15}O_1$, one input neuron, one hidden layer with fifteen neurons and one output neuron; (b) $I_2H_{15}O_1$, two input neurons, one hidden layer with fifteen neurons and one output neuron.

by $P_r = N_O + N_H (N_I + N_O + 1)$. Although MATLAB environment has the early stopping criterion to avoid overlearning, it is always advisable to get the relation $Pr/Tr < 1$. Hence, the number of neurons in the hidden layer was $N_H = 15$ to keep $Pr/Tr \ll 1$ for each simulated ANN with increasing the number of input layers from $N_I = 1$ to 11. The Early Stopping Criterion randomly divides the training dataset (T_r) in three categories: (1) training subset of the ANN (70% × T_r), (2) validation subset (15% × T_r) and (3) testing subset (15% × T_r). Data in the training subset were used to update the biases and weights of the ANN. Data in the validation subset were used to monitor the error after each training step and to stop the training process once the error in this validation subset started growing (indicating possible overlearning). Data in the testing subset were used as cross validation to compare different models, since they were not included in the training process.

First, the process of ranking the relevance of each input variable (X_1 to X_{11}) was initiated by training an ANN model with the $I_1H_{15}O_1$ structure for each one of the eleven candidate explanatory variables (X_1 to X_{11}) used as a single input variable (X_i in Fig. 3a). To overcome the uncertainty associated to the data selected for training, validating and testing, the bootstrapping technique with the 1 000 random resamples of the initial dataset was applied. The candidate variable X_i with the maximum coefficient of determination R^2 ($I_1H_{15}O_1$) in most of 1 000 resamples was considered the first relevant explanatory variable influencing wave reflection on mound breakwaters.

Second, the ANN model with the $I_2H_{15}O_1$ structure was considered, fixing the first relevant selected variable and varying the second input neuron with each candidate variable not previously selected ($\forall X_j \neq X_i$). Again, the second candidate variable associated to the maximum coefficient of determination R^2 ($I_2H_{15}O_1$) in most of the 1 000 resamples was considered the second relevant explanatory variable. This method was repeated for the eleven variables in Section 3 until R^2 barely improved with the inclusion of more variables (input neurons). Finally, after the ranking of the explanatory variables, simulations were conducted to develop the new empirical formula for wave reflection using only the most relevant explanatory variables.

5.2. Simulations to estimate the wave reflection

Fig. 4 shows the ranking of relevance of the explanatory variables affecting the wave reflection according to R^2 for each ANN model with a $I_{N_I}H_{15}O_1$ structure. For each step, the median value and 90% confident interval are given. It is observed that the relative water depth, h/L, was selected first as the most relevant variable with $R^2 = 0.91$, and the slope angle, $\cot\alpha$, was the second most relevant variable. Using h/L and $\cot\alpha$ as input variables in a $I_2H_{15}O_1$ model, the coefficient of determination is $R^2 = 0.99$ for the 265 UGR tests corresponding to regular waves, and R^2 does not significantly improve if other explanatory variables are included. Fig. 4 only shows the ranking variables from $N_I = 1$ to $N_I = 5$ since $N_I > 6$ did not improve the prediction.

Analyzing the 265 UGR tests with regular waves (A-UGR and B-UGR in Table 2), Fig. 5a shows the simulations of the ANN($I_1H_{15}O_1$) model using h/L as the only input variable. An exponential relationship is noted between h/L and the squared reflection coefficient, K_R^2. Eq. (15) is an explicit estimator of the squared reflection coefficient and 90% confident interval (assuming a Gaussian error distribution) corresponding to Fig. 5a with $R^2 = 0.84$,

$$K_R^2 = exp\left[-15.4\left(\frac{h}{L}\right)\right] \pm 0.074 \tag{15}$$

Using the ANN($I_2H_{15}O_1$) model as a function of h/L and $\cot\alpha$, the estimations for K_R^2 are shown in Fig. 5b. An exponential relationship with h/L is observed for each tested slope angle (A-UGR and B-UGR). Mild slopes have lower squared wave reflection coefficients. Eq. (16) provides the estimations and 90% confident interval (assuming a Gaussian error distribution) corresponding to Fig. 5b for $\cot\alpha = 1.5$ and $\cot\alpha = 2$ with $R^2 = 0.72$ and $R^2 = 0.83$, respectively.

$$K_R^2 = exp\left[-a\left(\frac{h}{L}\right)\right] \pm 0.076\ ;\ \begin{cases} being\ \ a = 13 & for\ \ \cot\alpha = 1.5 \\ being\ \ a = 16 & for\ \ \cot\alpha = 2.0 \end{cases} \tag{16}$$

To develop a simple relationship between the main explanatory variables and the squared reflection coefficient, different combinations of h/L and $\cot\alpha$ were considered, and a simple functional relationship was found: $(h/L) \bullet \cot\alpha = (h/L)/\tan\alpha$. Fig. 5c shows the estimations for the ANN($I_1H_{15}O_1$) model with the input variable $(h/L)/\tan\alpha$. Eq. (17)

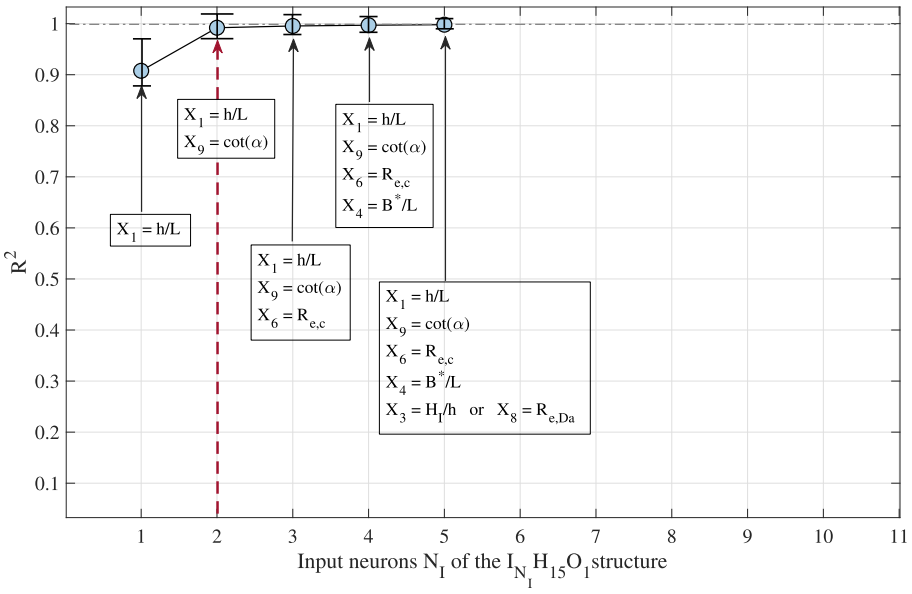

Fig. 4. Ranking of the candidate explanatory variables with the highest coefficient of determination, R^2, on the estimation of the squared reflection coefficient, K_R^2.

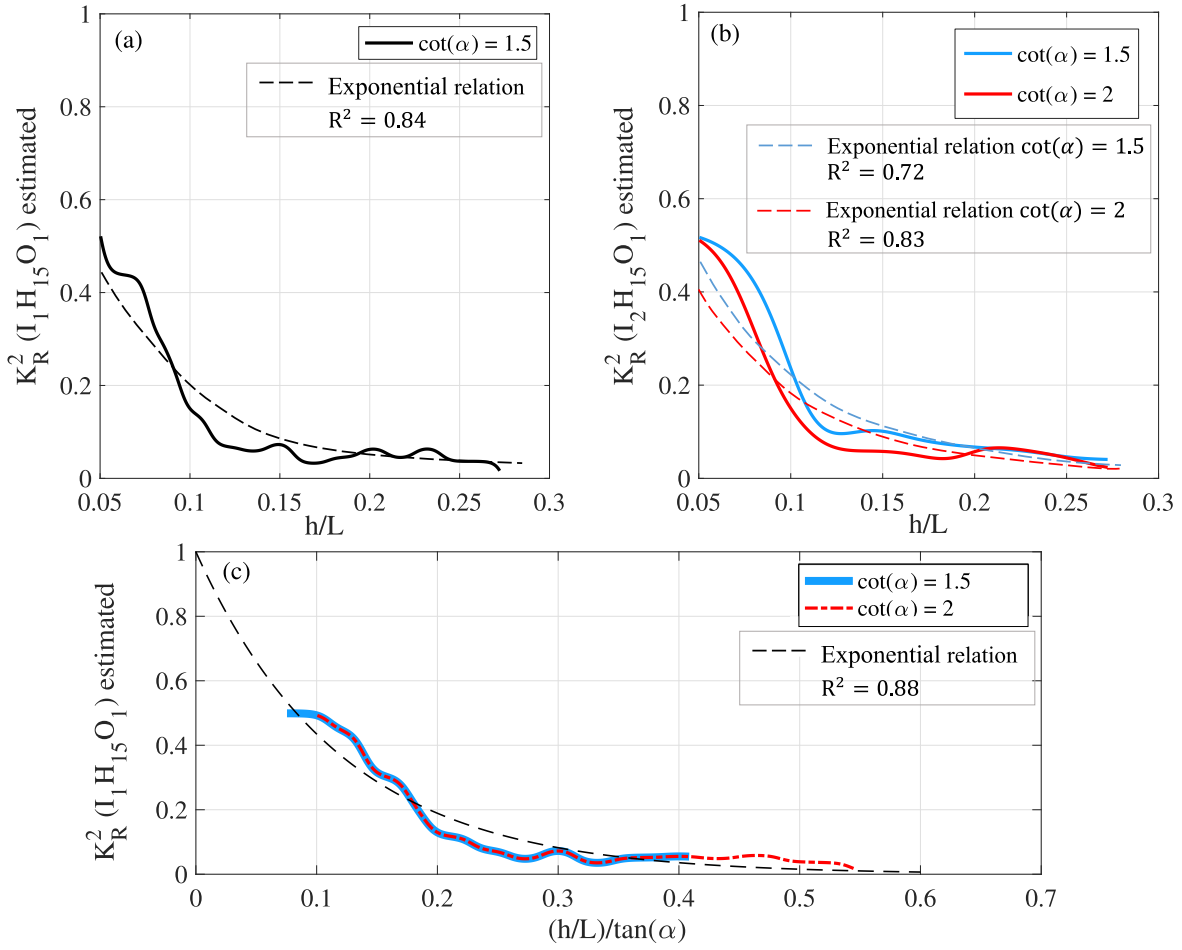

Fig. 5. Squared reflection coefficients given by: (a) ANN($I_1H_{15}O_1$) with input variable h/L, (b) ANN($I_2H_{15}O_1$) with input variables h/L and $\cot\alpha$, and (c) ANN ($I_1H_{15}O_1$) with input variable $(h/L)/\tan\alpha$. The solid lines and dashes represent the ANN estimations and the exponential relationship, respectively, between the explanatory variables and K_R^2 for the 265 A-UGR and B-UGR test with regular waves.

shows the estimations of K_R^2 for both tested slope angles (A-UGR and B-UGR) and 90% confident interval (assuming a Gaussian error distribution) with $R^2 = 0.88$,

$$K_R^2 = exp\left[-8\left(\frac{h/L}{tan\ \alpha}\right)\right] \pm 0.06 \quad (17)$$

Fig. 6 compares the measured and the estimated K_R^2 by Eq. (17) with a goodness of fit of $R^2 = 0.88$. It is observed that there are some structured residual values that could be fitted better with another type of relationship between the explanatory variables and K_R^2 and more fitting parameters; however, Eq. (17) not only has a high R^2 value but is simple and easy to apply. Eq. (17) is validated for conventional mound breakwaters with double-layer cube and rock armors, $1.5 \leq \cot\alpha \leq 2$, $0.05 \leq h/L \leq 0.028$, under regular waves, non-overtopping and non-breaking wave conditions.

5.3. Wave reflection formula for irregular waves

In this section, an ANN model is used to determine the best relationship between regular and irregular waves. This relationship was applied to the proposed wave reflection formula for regular waves (Eq. (17)) and then for 16 tests with irregular waves from the UGR dataset (*C*-UGR in Table 2). The root mean square incident wave height, $H_{rms,I}$, and spectral mean wave period, T_{01}, for irregular waves were compared with the wave height, H_I, and wave period, T, tested for regular waves in order to find the best λ_1 and λ_2 in $H_I = \lambda_1 \bullet H_{rms,I}$ and $T = \lambda_2 \bullet T_{01}$ to estimate K_R^2 in tests with irregular waves using Eq. (17).

Following the ANN methodology described in the previous section , an ANN($I_2H_3O_1$) model was developed to estimate K_R^2 valid for regular waves (106 tests corresponding to A-UGR in Table 2) with two input variables: the incident wave height, H_I, and wave period, T. This ANN ($I_2H_3O_1$) model was applied to the 16 tests with irregular waves using as input variables $H_I = \lambda_1 \bullet H_{rms,I}$ and $T = \lambda_2 \bullet T_{01}$. The values of λ_1 and λ_2 varied with a differential step of 0.001 in the ranges of $0.5 \leq \lambda_1 \leq 2.0$ and $0.8 \leq \lambda_2 \leq 1.5$. The best values for λ_1 and λ_2 are those that maximize R^2 between the K_R^2 estimated by ANN($I_2H_3O_1$) model and that measured from the 16 irregular waves (*C*-UGR tests in Table 2).

Fig. 7a compares the squared reflection coefficients estimated by ANN($I_2H_3O_1$) model and those measured from the 16 tests of *C*-UGR with irregular waves. The values of $\lambda_1 = 1.416$ and $\lambda_2 = 1.050$ for wave height and wave period, respectively, provide the best fit ($R^2 = 0.95$) between the estimated and measured K_R^2. These values of λ_1 and λ_2 correspond to the following relationship between the regular and irregular waves:

$$H_I \approx 1.416\ H_{rms,I} \approx H_{m0,I} \quad (18a)$$

$$T \approx 1.050\ \ T_{01} \quad (18b)$$

Fig. 7b shows the good agreement ($R^2 = 0.82$) between the K_R^2 estimated by Eq. (17) and that measured from the 16 tests with irregular waves (*C*-UGR). In Eq. (17), the wavelength at the toe of the structure for irregular waves, L_{01}, is calculated by applying the linear dispersion relationship with a wave period $T = 1.050\ T_{01}$.

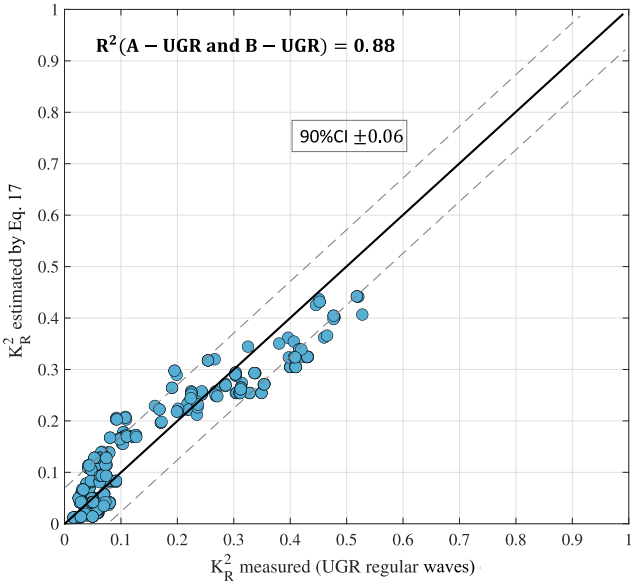

Fig. 6. Comparison between the squared reflection coefficients estimated by Eq. (17) and 90% confidence interval (CI) and the squared reflection coefficients measured in A-UGR and B-UGR tests (regular waves).

6. Validation of the new empirical formula for wave reflection on mound breakwaters

In this section, Eq. (17) developed to predict the proportion of wave reflection energy on mound breakwaters under non-overtopping and non-breaking wave conditions is validated using new experimental tests with irregular waves that were not used in the calibration process (blind test). Considering Eqs. (17) and (18), the following Eq. (19) is proposed with a 90% confident interval, assuming a Gaussian error distribution.

$$K_R^2 = exp\left[-8 \bullet \left(\frac{h/L_{01}}{tan\ \alpha}\right)\right] \pm 0.06;\ L_{01} = L\ (\mathrm{T} = 1.050\ T_{01}) \quad (19)$$

Fig. 8 illustrates the good agreement ($R^2 = 0.91$) between the K_R^2 estimated by Eq. (19) and that measured from the tests with irregular waves and various water depths performed at Aalborg University (tests D-AAU, *E*-AAU and F-AAU in Table 2). The physical models tested at AAU are mound breakwaters with double-layer cube and rock armors, $1.5 \leq \cot\alpha \leq 3$, different compositions of the core (permeable or impermeable) and relative water depths in the range $0.05 \leq h/L \leq 0.031$. Comparing Figs. 8 and 2, it is clear that the new empirical formula, Eq. (19), with only one explanatory variable fits the experimental data much better than the exiting estimation formulas described in Section 2 (see Table 1).

The AAU dataset was not used to estimate any parameter of Eq. (19) (only the UGR dataset was used). Moreover, the D-AAU and *E*-AAU datasets include tests with a slope angle $\cot\alpha = 3$ outside the calibration range of Eq. (17). This blind test with 91% of the variance explained ($R^2 = 0.91$) for the variety of AAU tests with irregular waves indicates the robustness of the new empirical formula.

As discussed in Section 2, Zanuttigh et al. (2013) proposed an ANN model to predict wave reflection from coastal and harbor structures using a database that included (1) part of the DELOS wave transmission database, (2) part of the CLASH wave overtopping database, (3) data from several European facilities, (4) field measurements and (5) tests on low-crested structures. Fig. 9 shows K_R^2 calculated with existing formulas, Eqs. 3, 4, 7, 8 and 10 (Table 1), and the new simple empirical formula, Eq. (19), compared to the K_R^2 measured from the database given in Zanuttigh et al. (2013), specifically Group G (223 tests with rock armor and a permeable core) and Group H (687 tests with concrete armor and a permeable core). The data selected from the Zanuttigh et al. (2013) database were breakwaters with straight slopes under non-overtopping and non-breaking wave conditions.

The new formula to estimate K_R^2 (Eq. (19)) has the best agreement for both Group G data (rock permeable) and Group H data (concrete permeable), although the agreement is not as good as that observed with the AAU data. Note that the database of Zanuttigh et al. (2013) is very extensive with laboratory tests conducted under very specific conditions, focusing mostly on overtopping and armor damage studies. Moreover, several concrete armor unit types other than cube armors are included in Fig. 9. The poor estimations of K_R^2 by some existing formulas

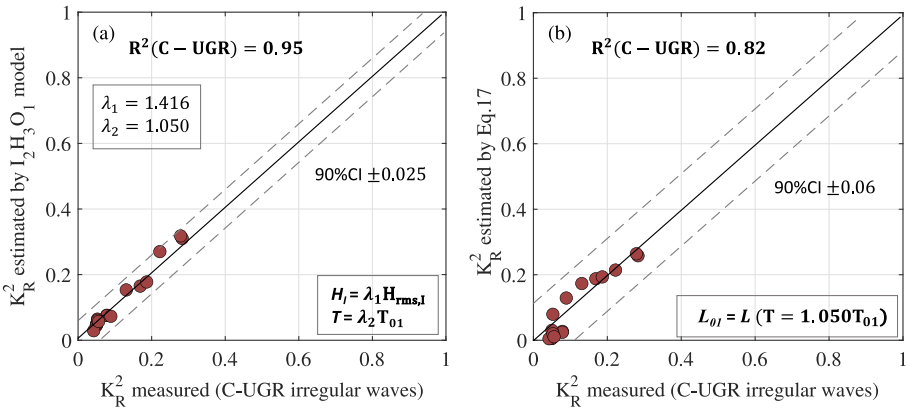

Fig. 7. Squared reflection coefficients measured from 16 tests with irregular waves (*C*-UGR in Table 2) compared with those estimated by: (a) ANN($I_2H_3O_1$) model to obtain the appropriate values of λ_1 and λ_2 corresponding to a relationship between regular and irregular waves, $H_I = \lambda_1 \bullet H_{rms,I}$ and $T = \lambda_2 \bullet T_{01}$; (b) empirical formula Eq. 17.

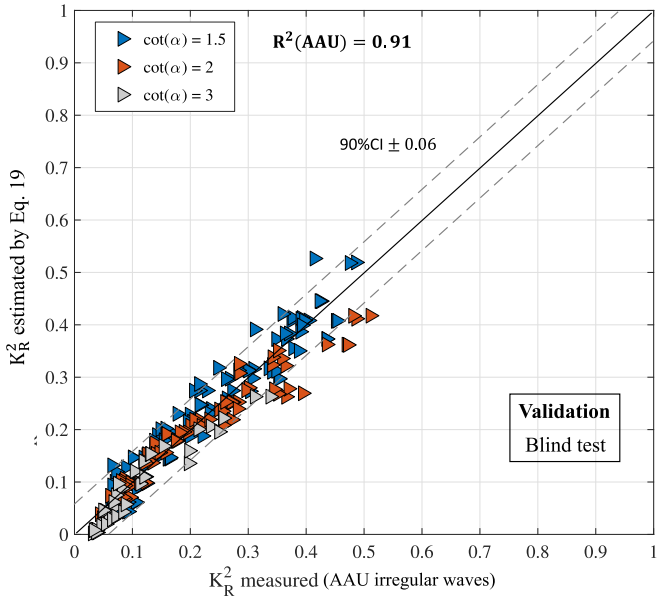

Fig. 8. Validation of the new empirical formula in a blind test. Squared reflection coefficients estimated by Eq. (19) and 90% confidence interval (CI) compared to squared reflection coefficients measured at AAU (irregular waves D-AAU, *E*-AAU and F-AAU in Table 2).

may be due to the application of said formulas outside their calibration range. For example, the Zanuttigh et al. (2013) database included data from Pearson et al. (2004) with concrete armors of Antifer, Tetrapods, X-blocks, Core-Locs, Haros and Dolos, which are unit types not included in the calibration of the current existing formulas. Eq. 4 b y Postma (1989) overestimates the results of concrete armor data as this formula was tested only for rock armors. Eq. 10 b y Medina and Gómez-Martín (2016) has a low R^2 value as their wave reflection formula was tested only for Cubipod® armor. Note that, although the data was filtered from the complete database provided by Zanuttigh et al. (2013), this database is very extensive with laboratory tests conducted under a variety of conditions and focused mostly on overtopping studies.

7. Conclusions

The main objective of this study was to develop a new one-parameter explicit formula to estimate wave reflection valid for conventional mound breakwaters under regular and irregular waves in non-overtopping and non-breaking wave conditions. An Artificial Neural Network (ANN) methodology was used to rank the influence of eleven candidate explanatory variables and to estimate the relationships between the explanatory variables and the squared wave reflection coefficient, K_R^2. A conventional empirical formula with only one parameter and one explanatory variable was calibrated using results from laboratory tests performed at the University of Granada (UGR) with regular waves on mound breakwaters with double-layer cube and rock armors, permeable cores and seaward slopes in the range $1.5 \leq \cot\alpha \leq 2$. Simulations of an ANN model were used to build up the new formula. To apply the proposed formula to irregular wave conditions, the best relationships for wave height and wave period, corresponding to regular and irregular waves, were obtained from an ANN model related to 16 tests with irregular waves from UGR. The blind test to validate the proposed formula for K_R^2 used the laboratory tests from Aalborg University (AAU) with irregular waves and conventional mound breakwaters with double-layer cube and rock armors, with and without filter layer, two core compositions (permeable and impermeable) and seaward slopes in the range $1.5 \leq \cot\alpha \leq 3$. Additionally, the performance of the new formula was compared to other formulas with 2 fitting parameters found in the literature, using the database given in Zanuttigh et al. (2013).

The application of the ANN methodology to the experimental test with regular waves from UGR allowed eleven selected potential explanatory variables to be ranked and used to estimate wave reflection on mound breakwaters under non-overtopping and non-breaking wave conditions. The relative water depth, h/L, and the seaward slope angle, cot α, explained 99% of the variance in the squared reflection coefficient, K_R^2. An exponential relationship with only one fitting parameter is proposed (Eq. (17)) and relates K_R^2 as a function of $(h/L)\ /\tan\alpha$. This 1-parameter empirical formula (Eq. 17) estimated K_R^2 with a coefficient of determination $R^2 = 0.88$ using the 265 tests with regular waves from UGR dataset.

The new proposed formula (Eq. (17)) to estimate K_R^2 for regular waves is also valid for irregular wave conditions by calculating the wavelength, L, as $L_{01} = L\ (T = 1.050\ T_{01})$. Eq. (19) is proposed as a new empirical and explicit formula to estimate K_R^2 for irregular waves and explained the 91% of the variance of K_R^2 measured in the AAU experimental tests with irregular waves. Eq. (19) was also applied to the data corresponding to conventional mound breakwaters in the extensive general database provided by Zanuttigh et al. (2013) allowing for better estimations than the 2-parameter formulas given in the literature (Eqs. 3, 4, 7, 8 and 10) with $R^2 = 0.65$ and $R^2 = 0.73$ for rock- and concrete unit-armored breakwaters, respectively. This is a remarkably good result for a new empirical formula with only one fitting parameter and only

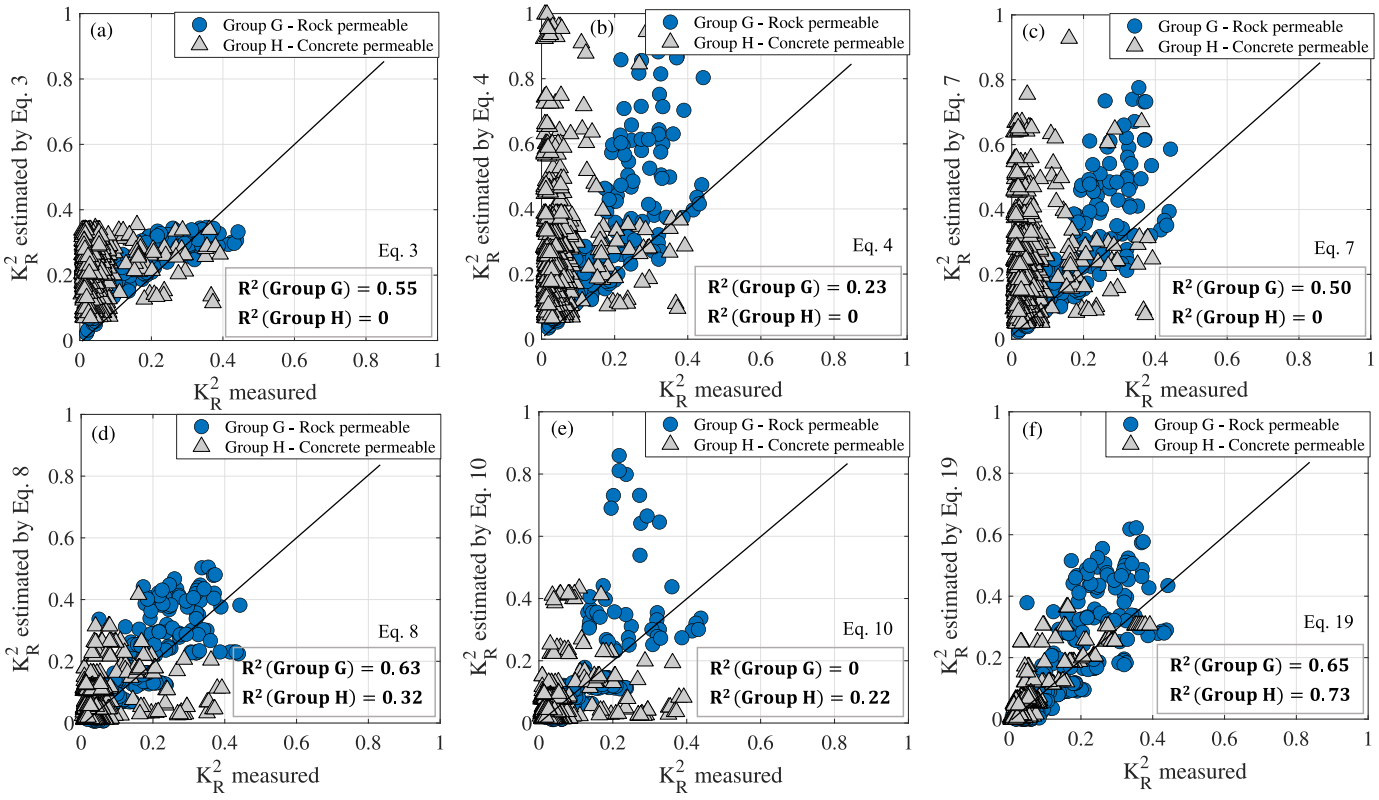

Fig. 9. Comparison between K_R^2 measured from the Zanuttigh et al. (2013) dataset with irregular waves (Group G – Rock permeable, Group H – Concrete permeable) and K_R^2 estimated by existing formulas with 2 parameters (Eqs. 3, 4, 7, 8 and 10) and the new empirical formula proposed in this study (Eq. (19)).

one explanatory variable $(h/L)/\tan\alpha$.

The new empirical formulas, Eqs. (17) and (19) for regular and irregular waves, respectively, are the simplest (only one explanatory variable and only one fitting parameter) formulas which significantly improves the estimations of wave reflection of conventional mound breakwaters under non-overtopping and non-breaking wave conditions. Eqs. (17) and (19) are valid for mound breakwaters with different armor unit types (cube and rocks), core permeabilities, seaward slope angles in the range $1.5 \leq \cot\alpha \leq 3$ and relative water depths in the range $0.05 \leq h/L \leq 0.031$. Outside this range of variables and mound breakwater characteristics, the proposed formulas should be used with caution.

CRediT authorship contribution statement

Pilar Díaz-Carrasco: Conceptualization, Funding acquisition, Formal analysis, Data curation, Writing – original draft, Writing – review & editing. **Jorge Molines:** Conceptualization, Writing – original draft, Writing – review & editing. **M. Esther Gómez-Martín:** Funding acquisition, Writing – review & editing. **Josep R. Medina:** Conceptualization, Funding acquisition, Writing – original draft, Writing – review & editing.

Declaration of competing interest

The authors declare that they have no known competing financial interests or personal relationships that could have appeared to influence the work reported in this paper.

Data availability

Data will be made available on request.

Acknowledgements

The first author is funded through the Juan de la Cierva 2020 program (FJC 2020-044778-I) by "*Unión Europea – NextGenerationEU en el marco del Plan de Recuperación, Transformación y Resiliencia de España*", Spanish Ministry of Science and Innovation. This work is supported by two projects (1) PID 2021-126475OB-I00 and (2) PID 2021-128035OA-I00, funded by the Spanish Ministry of Science and Innovation (FEDER, UE). The authors thank Prof. Thomas Lykke Andersen and Dr. Mads Røge Eldrup for providing the experimental data performed at the laboratory of Aalborg University. The authors also thank Prof. Barbara Zanuttigh and Dr. Sara M. Formentin for providing the database described in Zanuttigh et al. (2013), EurOtop et al. (2016), Zanuttigh et al. (2016) and Formentin et al. (2017). The manuscript was revised by Dr. Debra Westall (Universitat Politècnica de València, Spain).

List of symbols

A	fitting parameter of wave reflection formulas
A_{eq}	$\approx B_s \bullet h$, permeable core area under the still water level
b	fitting parameter of wave reflection formulas
B*	characteristic width of the core

B_s	width of the breakwater under the still water level
$D_{n50,a}$	nominal main armor diameter
$D_{n50,c}$	nominal core diameter
E_I	energy of the incident wave train
E_R	energy of the reflected wave train
F_{MT}	breakwater height
g	gravity
G_C	crest width
h	water depth
H	wave height, H =
H_I	for regular waves, H= $H_{rms,I}$ for irregular waves
H_I	incident wave height for regular waves
$H_{m0,I}$	significant spectral incident wave height
$H_{rms,I}$	root mean square incident wave height
$H_{rms,R}$	root mean square reflected wave height
H_R	reflected wave height
K_R^2	wave reflection coefficient
K_{R0}	fitting parameter of sigmoid function – lower asymptote
K_{R1}	fitting parameter of sigmoid function – upper asymptote
L	wavelength at the toe of the structure calculated with T
L_0	deep wavelength calculated with peak wave period
L_{01}	wavelength at the toe of the structure calculated with mean wave period, T_{01}
$L_{-1,0}$	the wavelength calculated with the spectral energy period, $T_{-1,0}$
n_p	core porosity
N_H	number of hidden layers
N_I	number of input layers
N_O	number of output layers
P	notional permeability factor
$R_{e,c}$	grain Reynolds number
$R_{e,Da}$	armor Reynolds number
R^2	coefficient of determination
T	wave period, T =
T	for regular waves, T = T_{01} for irregular waves
$T_{-1,0}$	spectral energy wave period
T_{01}	spectral mean wave period
T_p	peak wave period
U	characteristic seepage velocity
X_i "i"	explanatory variable
α	seaward slope angle
χ	similarity parameter defined by Díaz-Carrasco et al. (2020)
γ	fitting parameter of sigmoid function
ξ	Iribarren number calculated with wavelength at the toe of the structure
ξ_0	peak Iribarren number calculated with deep wavelength
$\xi_{-1,0}$	Iribarren number calculated with spectral energy wave period
ρ	water density
ν	kinematic water viscosity

References

Baquerizo, A., 1995. Reflexión del oleaje en playas. In: Métodos de evaluación y de predicción (PhD thesis). University of Cantabria (Spain).

Battjes, J.A., 1974. Surf similarity. In: Proceedings of 14th International Conference on Coastal Engineering, pp. 466–480. ASCE.

Benedicto, M.I., 2004. Comportamiento y evolución de la avería de los diques de abrigo frente a la acción del oleaje (PhD thesis). University of Granada (in Spanish).

Burcharth, H.F., Andersen, O.K., 1995. On the one-dimensional steady and unsteady porous flow equations. Coast. Eng. 24, 233–257.

Calabrese, M., Di Pace, P., Buccino, M., 2010. Wave reflection at rubble mound breakwaters ranging from submerged to exposed. In: Proc. Of 31st International Conference on Coastal Engineering. Hamburg, Germany.

Camus, P., Tomás, A., Díaz-Hernández, G., Rodríguez, B., Izaguirre, C., Losada, I.J., 2019. Probabilistic assessment of port operation downtimes under climate change. Coast. Eng. 147, 12–24.

CIRIA/CUR/CETMEF, 2007. The Rock Manual. The Use of Rock in Hydraulic Engineering. CIRIA, London (UK), p. C683, 2nd edition.

Clavero, M., Folgueras, P., Díaz-Carrasco, P., Ortega-Sánchez, M., Losada, M.A., 2018. A similarity parameter for breakwaters: the modified Iribarren number. In: Proceedings of 36th International Conference on Coastal Engineering. Baltimore, Maryland (USA).

Clavero, M., Díaz-Carrasco, P., Losada, M.A., 2020. Bulk wave dissipation in the main layer of slope rock and cube armored breakwaters. J. Mar. Sci. Eng. 8 (3), 152.

Davidson, M., Bird, P., Bullock, G., Huntley, D., 1996. A new non-dimensional number for the analysis of wave reflection from rubble mound breakwaters. Coastal Eng. Proc. 28, 93–120.

De Rouck, J., Geeraerts, J., 2005. Clash — final CLASH-report. Full Sci. Tech. Rep. www.clash-eu.org.

Díaz-Carrasco, P., 2019. Water-wave Interaction with Mound Breakwaters: from the Seabed to the Armor Layer. Ph.D. thesis. University of Granada (Spain).

Díaz-Carrasco, P., Moragues, M.V., Clavero, M., Losada, M.A., 2020. 2D Water-wave interaction with permeable and impermeable slopes: dimensional analysis and experimental overview. Coast. Eng. 158, 103682.

Díaz-Carrasco, P., Eldrup, M.R., Andersen, T.L., 2021. Advance in wave reflection estimation for rubble mound breakwaters: the importance of the relative water depth. Coast. Eng. 168.

Eldrup, M., Lykke Andersen, T., 2019a. Extension of shallow water rock amour stability formulae to nonlinear waves. J. Waterw. Port, Coast. Ocean Eng. 145 (1).

Eldrup, M., Lykke Andersen, T., 2019b. Estimation of incident and reflected wave trains in highly nonlinear two dimensional irregular waves. Coast. Eng. 153, 103536.

Eldrup, M., Lykke Andersen, T., Burcharth, H., 2019. Stability of rubble mound breakwaters - a study of the notional permeability factor, based on physical model tests. Water 934, 11.

EurOtop, 2016. In: van der Meer, J.W., Allsop, N.W.H., Bruce, T., DeRouck, J., Korthenhaus, A., Pullen, T., Schüttrumpf, H., Troch, P., Zanuttigh, B. (Eds.), Manual on Wave Overtopping of Sea Defenses and Related Structures. An Overtopping Manual Largely Based on European Research, but for Worldwide Application, second ed.

Formentin, S.M., Zanuttigh, B., Van der Meer, J.W., 2017. A Neural Network tool for predicting wave reflection, overtopping and transmission. Coast Eng. J. 59 (No. 2), 31, 1750006.

Garrido, J.M., Medina, J.R., 2012. New Neural Network-derived empirical formulas for estimating wave reflection on Jarlan-type breakwaters. Coast. Eng. 62, 9–18.

Gu, Z., Wang, H., 1991. Gravity waves over porous bottom. Coast. Eng. 15, 497–524.

Iribarren, C.R., Nogales, C., 1949. Protection des ports. In: 17th International Navigation Congress of PIANC. S.II – C.4 Lisbon (Portugal).

Kortenhaus, A., Oumeraci, H., 1998. Classification of wave loading on monolithic coastal structures. Coast. Eng. 26, 867–880.

Lara, J.L., Garcia, N., Losada, I.J., 2006. RANS modelling applied to random wave interaction with submerged permeable structures. Coast. Eng. 53, 395–417.

Losada, M., Giménez-Curto, L.A., 1981. Flow characteristics on rough, permeable slopes under wave action. Coast. Eng. 4.

Lykke Andersen, T., Burcharth, H.F., 2004. CLASH Work Package 4.4–D24. Report on Additional Tests. Part D Berm Breakwater Tests (On-line available).

Mansard, E.P.D., Funke, E.R., 1987. On the reflection analysis of irregular waves. In: Natl. Res. Cunc. Rev. Can. Hydraulics Laboratory Technical Report. TR-HY-O17.

Mares-Nasarre, P., Molines, J., Gómez-Martín, M.E., Medina, J.R., 2021. Explicit Neural Network-derived formula for overtopping Flow on mound breakwaters in depth-limited breaking wave conditions. Coast. Eng. 164, 103810.

MATLAB, 2022. MATLAB®2022a. The MathWorks Inc. Natick, MA.

Medina, J.R., Gómez-Martín, M.E., 2016. Cubipod® Manual. Universitat Politècnica de València, Valencia.

Molines, J., Medina, J.R., 2016. Explicit wave overtopping formula for mound breakwaters with crown wall using CLASH Neural Network derived data. J. Waterw. Port, Coast. Ocean Eng. 142 (3), 04015024.

Molines, J., Herrera, M.P., Medina, J.R., 2018. Estimations of wave forces on crown walls based on overtopping rates. Coast. Eng. 132, 50–62.

Muttray, M., Oumeraci, H., Ten Oever, E., 2006. Wave Reflection and Wave Run-Up at Rubble Mound Breakwaters. Proc. of XXX ICCE, San Diego, California.

Numata, A., 1976. Laboratory formulation for transmission and reflection at permeable breakwaters of artificial blocks. Coast. Eng. Jpn. 19 (1), 47–58.

Pearson, J., Bruce, T., Franco, L., Van der Meer, J.W., 2004. Report on Additional Tests, Part B, CLASH WP4 Report. University of Edinburgh, Edinburgh, UK.

Pérez-Romero, D.M., Ortega-Sánchez, M., Moñino, A., Losada, M.A., 2009. Characteristic friction coefficient and scale effects in oscillatory flow. Coast. Eng. 56, 931–939.

Postma, G.M., 1989. Wave Reflection from Rock Slopes under Random Wave Attacks. PhD thesis) Delft University of Technology.

Requejo, S., Vidal, C., Losada, I.J., 2002. Modeling of wave loads and hydraulic performance of vertical permeable structures. Coast. Eng. 46, 249–276.

Riedel, H.P., Byrne, A.P., 1986. Random breaking waves – horizontal seabed. In: Proceedings of 20th International Conference on Coastal Engineering. Taipei, Taiwan.

Seelig, W.N., Ahrens, J.T., 1981. Estimation of wave reflection and energy dissipation coefficients for beaches, revetments and breakwaters. In: CERC Technical Paper 811. Fort Belvoir. U.S.A.C.E, Vicksburg, MS.

University, Aalborg, 2015. Wave Data Acquisition and Analysis Software – WaveLab 3. Aalborg University. Department of Civil Engineering. http://www.hydrosoft.civil.aay.dk/wavelab/.

Van der Meer, J.W., 1988. Rock slopes and gravel beaches under wave attack. In: Doctoral Thesis) Also Delft Hydraulics. Delft University of Technology. Publication no. 396.

Van der Meer, J., 1992. Conceptual design of rubble mound breakwaters. proc. of a short course on the design and reliability of coastal structures. In: XXIII International Conference Coastal Engineering Tecnoprint, pp. 447–510. Venice.

Van Gent, M.R., 1995. Wave Interaction with Permeable Coastal Structures. Ph.D. thesis. Delft University.

Van Gent, M.R.A., Van den Boogaard, H.F.P., Pozueta, B., Medina, J.R., 2007. Neural network modelling of wave overtopping at coastal structures. Coast. Eng. 54 (8), 586–593.

Vílchez, M., Clavero, M., Losada, M.A., 2016. Hydraulic performance of different non-overtopped breakwater types under 2d wave attack. Coast. Eng. 107, 34–52.

Wurjanto, A., Kobayashi, N., 1993. Irregular wave reflection and runup on permeable slopes. J. Waterw. Port, Coast. Ocean Eng. 119 (5), 537–557.

Zanuttigh, B., Lykke Andersen, T., 2010. Wave reflection in 3D conditions. Coast. Eng. 57, 531–538.

Zanuttigh, B., Van der Meer, J., 2008. Wave reflection from coastal structures in design conditions. Coast. Eng. 55, 771–779.

Zanuttigh, B., Van der Meer, J.W., Lykke Andersen, T., Lara, J.L., Losada, I.J., 2009. Analysis of Wave Reflection from Structures with Berms through an Extensive Database and 2DV Numerical Modelling, vol. 4. Proc. of XXXI ICCE, Hamburg, Germany, pp. 3285–3297.

Zanuttigh, B., Formentin, S.M., Briganti, R., 2013. A Neural Network for the prediction of wave reflection from coastal and harbor structures. Coast. Eng. 80, 49–67.

Zanuttigh, B., Formentin, S.M., Van der Meer, J.W., 2016. Prediction of extreme and tolerable wave overtopping discharges through an advanced Neural Network. Ocean Eng. 127, 7–22.